ELSEVIER

Polymer 41 (2000) 8741–8747

polymer

www.elsevier.nl/locate/polymer

Polymer Communication

Molecular dynamics studies of the thermodynamics of HDPE/butene-based LLDPE blends

P. Choi*

Department of Chemical and Materials Engineering, University of Alberta, Edmonton, Alta., Canada T6G 2G6

Received 15 September 1999; received in revised form 7 November 1999; accepted 10 March 2000

Abstract

Hildebrand solubility parameters (δ) at elevated temperatures were computed for models of high-density polyethylene (HDPE) and a series of butene-based linear low-density polyethylene (b-LLDPE) with different branch contents using molecular dynamics simulation. And the δ values were then used to calculate the corresponding Flory–Huggins interaction parameter (χ) between HDPE and various b-LLDPE models. The results indicate that the level of branch content of b-LLDPE that is required to phase separate the blends in the liquid state is about 40 branches/1000 backbone carbons, regardless of temperature. This is consistent with the recent small angle neutron scattering (SANS) findings of Alamo et al. [Macromolecules 1997;30:561–566]. © 2000 Elsevier Science Ltd. All rights reserved.

Keywords: HDPE; Butene-based LLDPE; Branch content

1. Introduction

Polyethylene–polyethylene miscibility has been a topic of great academic and commercial interest for the past decade, owing to its relevancy to the understanding of processing and performance properties of blends containing different types of polyethylenes. Despite considerable efforts that have been made to the subject, a consensus has not yet been achieved concerning the liquid–liquid miscibility of such blends. For example, different groups of researchers have proposed completely opposite views ranging from total phase separation [1–8] to complete homogeneity [9–11] for blends composed of high-density polyethylene (HDPE) and low-density polyethylene (LDPE) as well as HDPE and linear low-density polyethylene (LLDPE). Nevertheless, in the case of HDPE/LLDPE blends, researchers have demonstrated unanimously that the average number of branches per thousand backbone carbons (i.e. the branch content) of LLDPE is the major molecular factor that controls miscibility [6–8,10,12]. In particular, using small angle neutron scattering (SANS), Alamo et al. [10] have shown that if the branch content of LLDPE is below 40, HDPE and LLDPE form homogenous mixtures. However, when the branch content is higher than 80, the blends phase separate. But the authors made no comments on the miscibility of such blends with branch contents of LLDPE intermediate between 40 and 80. On the other hand, using transmission electron microscopy (TEM), Hill et al. [6–8,12] have shown that the threshold value for the same blends is about 60.

To a certain extent, the branch content effect is not totally unexpected since it is consistent with the Hildebrand solubility parameter formalism. It is well known that the solubility parameter is not only determined by the interaction energy potential, $u(r)$, but also the local arrangement of the molecules, $g(r)$, as depicted in the following expression:

$$\delta = \sqrt{\frac{\Delta E_v}{V}} = \sqrt{\frac{2\pi n^2}{V^2} \int_0^\infty u(r) g(r) r^2 \, \mathrm{d}r} \tag{1}$$

where δ is the Hildebrand solubility parameter; $\Delta E_v/V$ is the cohesive energy density; n is the number of molecules; $u(r)$ is the interaction energy potential; and $g(r)$ is the radial distribution function. As one can conceive, polyethylene with different branching characteristics and/or contents should exhibit different local liquid morphology (i.e. different $g(r)$). Therefore, it is not surprising that δ values of different polyethylenes can differ and such differences lead to liquid-liquid phase separation although the interactions between various segments are similar. In fact, recent theoretical studies of the miscibility of other polyolefin blends (e.g. polyethylene/polypropylene blends) based upon Polymer Reference Interaction Site Model (PRISM) theory and molecular modeling have suggested that miscibility of polyolefins is extremely sensitive to differences in

* Tel.: + 1-708-492-9018; fax: + 1-780-492-2881.
E-mail address: phillip.choi@ualberta.ca (P. Choi).

PII: S0032-3861(00)00279-2

Table 1
Descriptions of the model systems of polyethylene

Model	Branch content (branches per 1000 backbone carbons)	Molecular mass (g/mol)	Experimental density of polyethylene used for the simulations (g/cm^3)				
			425 K (152°C)	450 K (177°C)	475 K (202°C)	500 K (227°C)	525 K (252°C)
1	0	14,029					
2	10	14,310					
3	20	14,590					
4	40	15,151	0.779	0.766	0.753	0.740	0.728
5	50	15,432					
6	80	16,273					

the short-ranged local structures of the polymers [13–18]. In other words, in addition to differences in intermolecular interactions, their miscibility depends strongly on their packing disparities.

In this article, we report our recent molecular modeling results on the effect of branch content of butene-based LLDPE on its miscibility with HDPE. In particular, molecular dynamics simulation has been applied to compute δ values of models of HDPE and a series of butene-based LLDPE with different branch contents in the temperature range over which these polymers are usually processed. And the resulting δ values were then used to calculate their corresponding Flory–Huggins interaction parameter (χ) using the well-known expression derived by combining the Hildebrand solubility and Flory–Huggins lattice theories [19]:

$$\chi = \frac{V}{RT}(\delta_{HDPE} - \delta_{LLDPE})^2 \quad (2)$$

where V is the molar volume of the smallest monomer unit among the blend components. In this work, since both components are polyethylene, the experimental molar volumes of ethylene monomer unit at various simulation temperatures were used. The major reason for using the above expression for calculating χ is that it offers a computationally less demanding alternative because such an approach does not require simulation of the blends, only the pure components. Fortunately, both experimental studies and theoretical work have suggested that the above expression is valid for hydrocarbon polymer blends [20]. As a result, we feel justified for using such a simple approach for calculating χ.

2. Molecular dyanmcis simulation

Molecular dynamics (MD) simulations were carried out for six single-chain models of polyethylene using a molecular modeling software package Cerius 2, version 3.5, from Molecular Simulations Inc. Each model contained a skeletal chain composed of 500 ethylene monomer units (i.e. 1000 backbone carbons) with a fixed number of short branches composed of two carbons. The model without branches mimics the HDPE molecule while the others butene-based LLDPE. Since the branches distributed randomly along the skeletal chain, the model molecules resemble to LLDPE produced by Ziegler–Natta type of catalysts. The respective branch content was set at 10, 20, 40, 50, and 80 for each LLDPE model. The main reason for using long chains rather than short chains (e.g. 100 backbone carbon chains) is to capture the branch content effect with statistically representative models. Because of the size of the models, we chose a united-atom approach to reduce the computational efforts [21].

A Monte-Carlo algorithm, which is based upon the strategies developed by Theodorou and Suter [22] some years ago, was used to create the amorphous states of the models at elevated temperatures. In such procedure, a unit cell was first created for each molecular model using the experimental melt density and molecular mass of the chain being simulated. For example, the melt density of polyethylene, independent of the branch content [23], at 425 K and 0.1 MPa has a value of 0.779 g/cm^3 and the molecular mass of model 1 (see Table 1) is 14,029 g/mol. Therefore, the molar volume is approximately 17,974 cm^3/mol. Dividing the molar volume by Avorgadro's number would give the volume of one molecule. And the size of the cubic unit cell was then determined simply to be $31 \times 31 \times 31$ Å^3. The experimental melt density used for the simulations was calculated using an empirical expression developed by Rudin et al. [23] and is summarized in Table 1.

The algorithm then placed the midpoint of each chain randomly into the unit cell and the polymer structures were grown from the middle outwards. In this growing process, a hard core radius equivalent to 0.3 of the van der Waals radius of the united atoms was imposed to avoid hard overlaps. In addition, an inter-dependent rotational isomeric state (RIS) scheme [24] was used by which the distribution of any torsion of the skeletal chain was assigned using the known RIS states with an energy barrier of 4.186 kJ/mol and the torsion states of its neighboring bonds. The distribution of the torsion states was calculated based upon Bolztmann statistics and the chosen simulation temperature. For the carbon-carbon bonds in the branches, the distribution of the initial torsions was assigned in a random fashion since RIS states of those torsions are not available.

Table 2
Lennard-Jones parameters used for the simulations

United atom type	σ_0 (nm)	ϵ_0 (kJ/mol)
Carbon with one implicit hydrogen	0.3983	0.615
Carbon with two implicit hydrogens	0.4068	0.829
Carbon with three implicit hydrogens	0.4152	1.047

In addition to the above constraints, each unit cell is also subject to periodic boundary conditions [25]. The main advantage of imposing periodic boundary conditions is to reduce the number of atoms required to simulate the liquid state of polymers. In general, the initial conformations created using the above procedure are in a high-energy state. Energy minimizations were therefore carried out using a conjugate gradient method to relax all the structures before the high temperature MD annealings. In regard with modeling the intra and inter-molecular interactions, a generic force field, Dreiding 2.21, developed by Mayo et al. [26], was adopted on account of its simplicity and the availability of united-atom parameters. In Dreiding 2.21, like other classical force fields, the total potential energy of a polymer molecule is described as the summation of terms arising from the parameterization of the bonding and non-bonding interactions. For the systems of interest in the present work, van der Waals interactions, modeled by a Lennard-Jones 6-12 potential, were the only non-bonded interactions considered. Off diagonal van der Waals parameters are obtained using the geometric mean rule. The non-bonded interaction energy in the periodic cells was calculated using an Ewald procedure [25]. The corresponding Lennard-Jones parameters are summarized in Table 2. Harmonic potentials were used to model bond length and bond angle deformation. All equilibrium bond lengths and force constant used were 1.53 Å and 2930 kJ/mol/Å, respectively.

In any MD simulation, the selection of force field is of paramount importance. The force field we used has been found to be capable of reproducing δ values very accurately for a wide variety of non-ionic surfactants and non-polar small molecules [27–30]. In fact, δ values obtained in the present work agree very well with recent experimental results of Han et al. [31] on comparable polyethylene systems (see Results and Discussion). However, like many other force fields, Drieding 2.21 suffers from the same drawback that the calculated average pressures deviate significantly from the experimental values when NVT ensemble is used (see Table 3). It is not clear why accurate δ values were obtained while the calculated average pressures did not match with the expected value of 0.1 MPa (i.e. 1 atm) under which the experimental density was measured. Further investigation is required to resolve this issue. So far as we know, other research groups have also reported similar observations [32–34]. In particular, they found that average pressures obtained in the NVT simulations are generally within a range of approximately $\pm$300 atm from the experimental values. Nevertheless, since our main interest is in examining the effect of branch content on miscibility utilizing the computed δ values, we feel justified for not introducing pressure corrections.

Since united atom models do not give accurate density, we decided to carry out NVT, instead of NPT, MD simulation, based upon the scheme developed by Nosé [35] with a Leapfog numerical algorithm [25], for all models. In this way, the density, which has a strong influence on the liquid morphology of the models and the corresponding δ, can be controlled at the experimental values. Note that with the size of models and the number of MD runs required for the present study, NPT MD simulation is not practical. In general, for the same system, an NPT simulation requires much longer CPU time than that of an NVT simulation. The simulation temperatures were chosen at 425, 450, 475, 500 and 525 K and the simulation time was 1000 pico-seconds (ps) with a time step of 1 feto-second (fs) for all models. It is believed that the simulation time is long enough for the systems to relax and to achieve thermodynamic equilibrium. Once the MD trajectories were created, the total energy of the last 100 ps of each simulation was analyzed and used to compute δ of the systems. And the detailed procedure is described elsewhere [36].

Table 3
Average pressures (MPa) of the model systems obtained in the NVT simulations at various elevated temperatures (note that the pressure that corresponds to the experimental densities used in the present work is 0.1 MPa)

Model	Simulation temperature (°C)				
	152	177	202	227	252
1	−196 ± 31	−154 ± 30	−136 ± 29	−128 ± 30	−120 ± 27
2	−175 ± 27	−167 ± 29	−164 ± 29	−152 ± 30	−131 ± 31
3	−178 ± 30	−140 ± 28	−160 ± 29	−136 ± 27	−107 ± 24
4	−76 ± 21	−153 ± 36	−126 ± 30	−133 ± 29	−106 ± 29
5	−67 ± 23	−14 ± 28	−153 ± 26	−125 ± 31	−100 ± 31
6	−79 ± 20	−156 ± 28	−128 ± 26	−104 ± 24	−98 ± 25

Table 4
Computed Hildebrand solubility parameters, in $(MPa)^{1/2}$, of the model systems at various elevated temperatures

Model	Simulation temperature (°C)				
	152	177	202	227	252
1	18.6 ± 0.1	18.5 ± 0.2	17.8 ± 0.2	17.8 ± 0.1	17.1 ± 0.2
2	18.8 ± 0.1	17.7 ± 0.2	18.2 ± 0.2	17.2 ± 0.2	16.5 ± 0.2
3	18.4 ± 0.1	18.2 ± 0.1	17.2 ± 0.1	17.2 ± 0.2	16.7 ± 0.2
4	17.9 ± 0.2	17.4 ± 0.2	17.2 ± 0.2	16.9 ± 0.2	16.8 ± 0.2
5	17.5 ± 0.2	17.1 ± 0.2	16.8 ± 0.2	15.9 ± 0.2	14.9 ± 0.2
6	17.5 ± 0.2	17.2 ± 0.2	16.7 ± 0.2	15.5 ± 0.2	15.4 ± 0.2

3. Results and discussion

The computed δ values of the model systems of HDPE and butene-based LLDPE over the temperature range of 425 K to 525 K are summarized in Table 4. The ± values shown in Table 4 represent the ensemble fluctuations in the computed δ values for a given set of force field parameters and are not a computational error estimate. Their magnitudes, which are rather small, indicate that the MD calculations are highly reproducible and do not depend on the initial conformations used. As shown in the same table, the computed δ decreases with increasing temperature as well as with increasing branch content. Such trends are consistent with recent experimental observations of Han et al. [31]. The magnitudes of our interpolated δ values at 166°C are over the range of 17.3 ± 0.2 to 18.6 ± 0.1 $(MPa)^{1/2}$ which coincide with their δ values obtained from PVT measurements of comparable butene-based polyethylene systems under the conditions of 166°C and 0.1 MPa ($17.2–18.3$ $(MPa)^{1/2}$).

When the computed δ values were used to calculate χ between HDPE and various butene-based LLDPE models, irregular temperature dependence, as depicted in Fig. 1, was observed. This is not in accord with the original Flory–Huggins lattice theory because χ should exhibit an inverse temperature dependence if there is no change in volume on mixing. However, such behavior is somewhat expected because all χ was calculated using the δ values of the pure components that have a non-inverse temperature dependence. It is clear from the Eq. (1) that δ depends on both V and $g(r)$ that do not depend on temperature in an inverse fashion. In fact, other researchers have also reported such non-1/T temperature dependence of χ for other polyolefin blends using techniques such as SANS, cloud point determinations and PVT measurements [37–39].

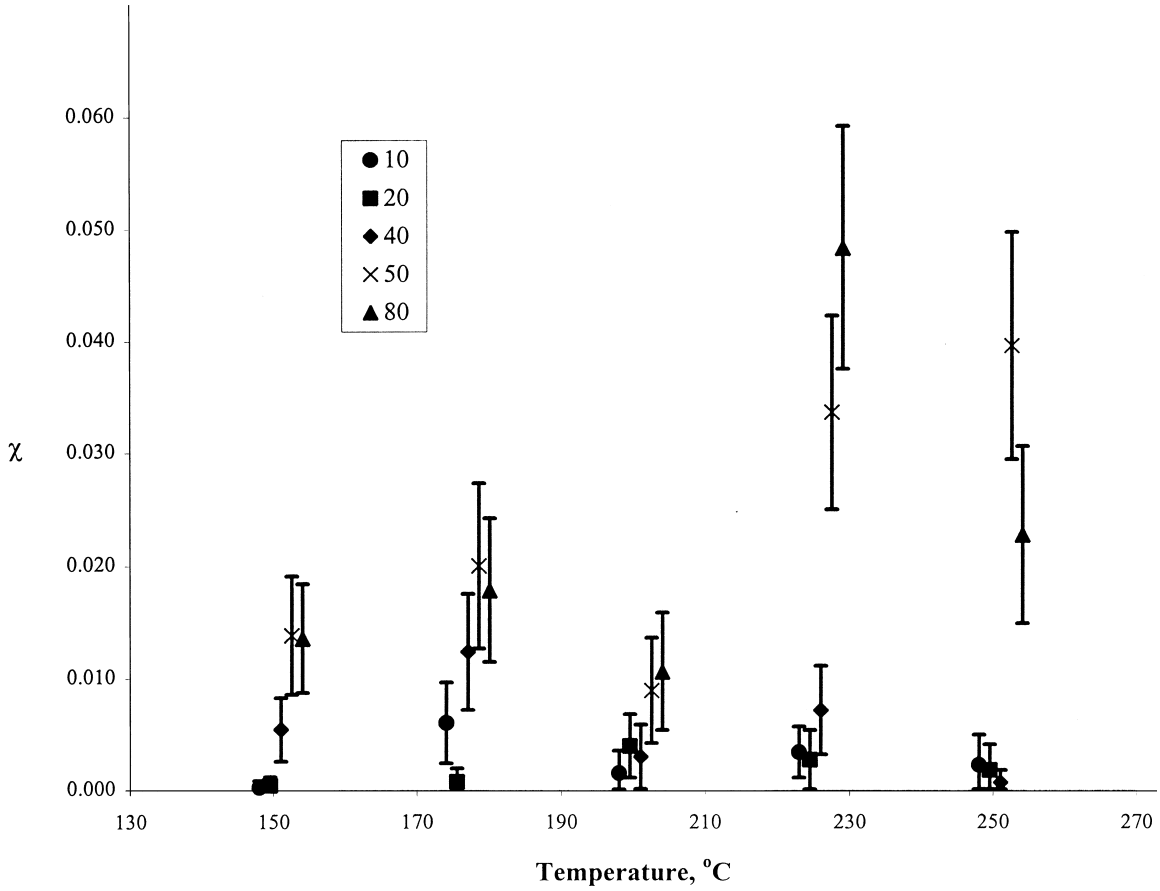

Fig. 1. Temperature dependence of χ for the blends composed of modeled HDPE and butene-based LLDPE with different branch contents. The data points and the corresponding standard deviations are shift horizontally for clarity.

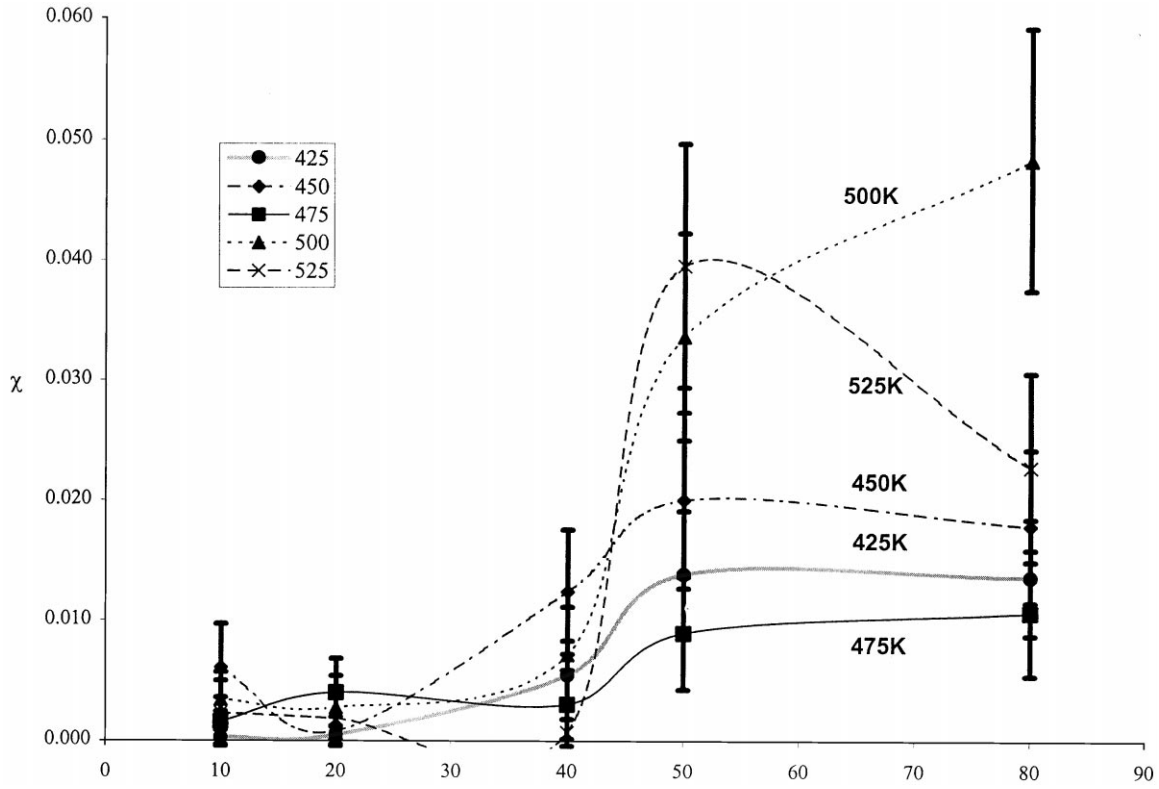

Fig. 2. The Flory–Huggins interaction parameter χ vs branch content of the butene-based LLDPE models at five elevated temperatures. The lines are drawn to guide the eye.

According to Fig. 1, when the branch content is low (i.e. less than 40), χ seems to have a week dependence on temperature and stays very close to zero, the critical interaction parameter χ_{critical}; deviates considerably from zero when the branch content is high. The deviation is more pronounced at higher temperatures indicating that the blends composed of HDPE and high branch content butene-based LLDPE may exhibit a LCST type of phase diagram. It was also observed that the $\pm$ values associated with the calculated χ are large when the branch content is high. Such observation is attributed to the large $\Delta\delta$ values obtained rather than the computational inaccuracy. It should be noted that the $\pm$ values associated the computed χ (i.e. dχ) were calculated using the following expression [40]:

$$\mathrm{d}\chi = \frac{2V\Delta\delta}{\mathrm{R}T}\mathrm{d}(\Delta\delta) \tag{3}$$

where V, $\Delta\delta$, R, and T carry the same meanings as defined earlier and d($\Delta\delta$) is the ensemble fluctuations of δ obtained from the MD calculations (i.e. the $\pm$ values associated with the average δ values). It is evident from the above expression that larger the $\Delta\delta$ is (even though d($\Delta\delta$) is very small), larger the dχ is. These statistical fluctuations are inherent in this type of calculations; therefore, there are no alternatives for reducing such quantities unless extremely small d($\Delta\delta$) values can be obtained. This, in turn, requires the use of larger molecular systems and number of MD runs that are practically impossible.

When the computed χ was plotted against the branch content, it is apparent in Fig. 2 that χ changes abruptly at a branch content of around 40 at all temperatures. And the change is more pronounced when the temperature is above 500 K. When the branch content is high, say 80, large positive χ values were obtained indicating that the polymers in question phase separate at all simulation temperatures. The results are consistent with the findings of Alamo et al. [10]. In fact, at low branch contents, the computed χ values are in good agreement with those obtained by the same authors.

It is worth noting that even though we used extremely simple models and force field parameters, the data reproduce remarkably well the experimentally observed cutoff branch content values determined by the experimentalists. These results reinforce once again that the solubility parameter formalism, although simple, can be used to describe the thermodynamics of blend systems containing polyethylenes effectively. The results also suggest that polyethylenes with different molecular architectures are not necessarily thermodynamically miscible especially when the branch contents of them differ considerably. It is evident from the present work that such differences can lead to large $\Delta\delta$ or χ values that promote liquid–liquid phase separation. In consistent with findings of other researchers [13–18], such

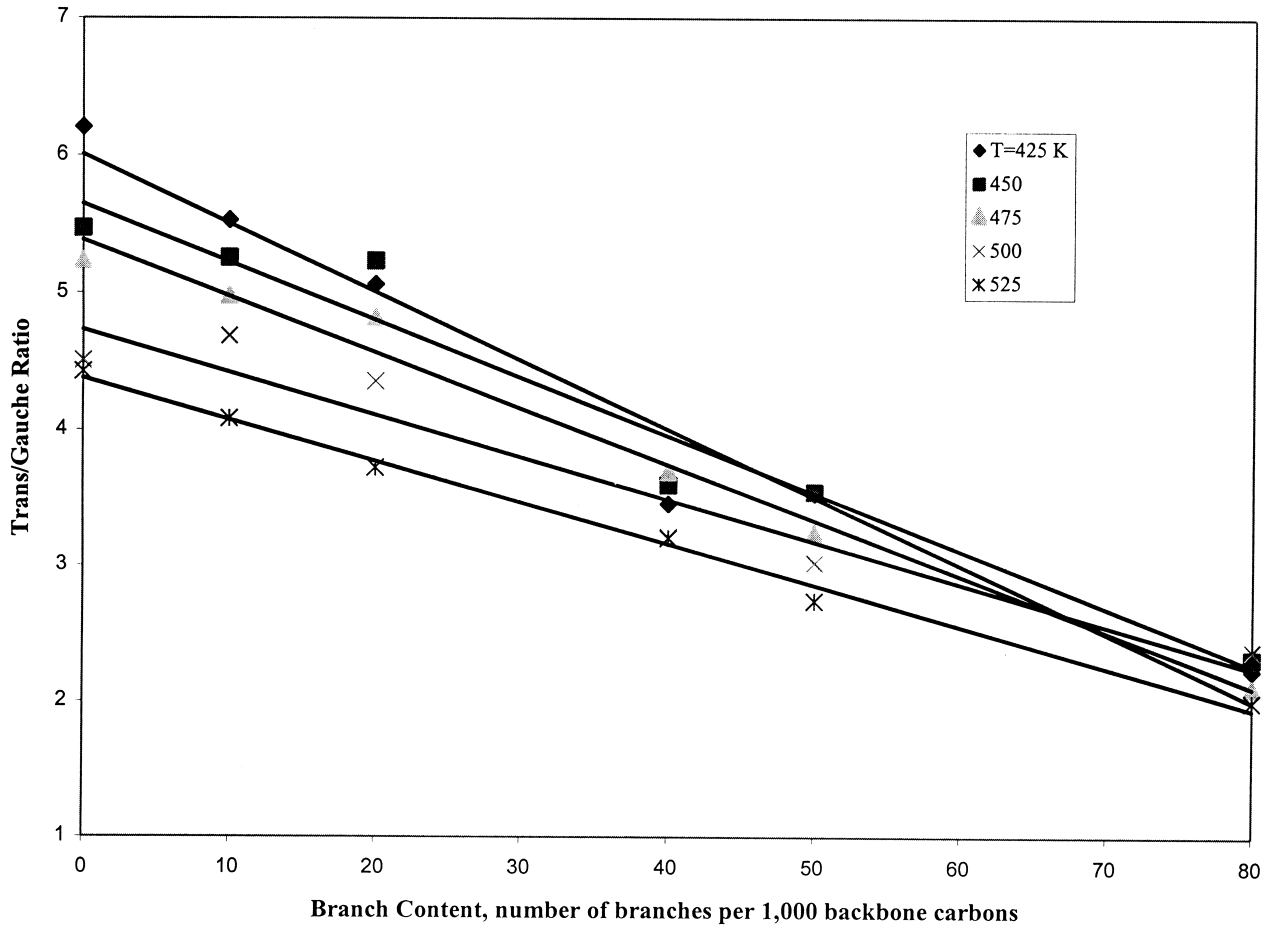

Fig. 3. Branch content dependence of trans/gauche ratio for the polyethylene models at five elevated temperatures. The lines are drawn to guide the eye.

large $\Delta\delta$ is attributed to the differences in the local arrangements of different polyethylene molecules. This can be illustrated by plotting the *trans*/*gauche* ratio of the backbone torsions (t/g ratio) as a function of branch content (see Fig. 3). Note that t/g ratios are used here rather than $g(r)$ since $g(r)$ of the modeled systems resemble to each other, a consequence of united atom models. In light of Figs. 2 and 3, it is obvious that the larger the differences in the t/g ratios, the larger the $\Delta\delta$ value. However, with the present data, we cannot rule out the importance of $u(r)$ because by adding more branches (i.e. more CH_3 and CH groups) to the skeletal chain of LLDPE molecules, one introduces more non CH_2–CH_2 interactions between HDPE and LLDPE molecules. Further investigation is needed to de-convolute the packing effects and interaction energy on the miscibility issue.

In summary, we have demonstrated that the phase behavior of blends composed of HDPE and butene-based LLDPE can be described in the framework of Hildebrand solubility parameter formalism. Even with the use of highly simplified molecular models and a generic force field, we have been able to reproduce the SANS or TEM observation that the branch content of butene-based LLDPE plays an important role in determining its miscibility with HDPE. In particular, when the branch content is high (i.e. >40), the polymers phase separate, and such phase separation becomes even more pronounced when the temperature is higher. In the future, we will examine the effects of branch length and co-monomer distribution on miscibility of such blends.

Acknowledgements

The author would like to thank the Natural Science and Engineering Research Council of Canada for financial support of this work through an equipment grant, as well as Thomas Man, Astral Man, and Jerry Fan for performing the data analysis and preparing the graphs.

References

[1] Barham PJ, Hill MJ, Keller A, Rosney CCA. J Mater Sci Lett 1988;7:1271–5.
[2] Hill MJ, Barham PJ, Keller A, Rosney CCA. Polymer 1991;32(8):1384–93.
[3] Hill MJ, Barham PJ, Keller A. Polymer 1992;33(12):2530–51.
[4] Hill MJ, Barham PJ. Polymer 1992;33(19):4099–107.
[5] Hill MJ. Polymer 1994;35(9):1991–3.

[6] Hill MJ, Barham PJ, van Ruiten J. Polymer 1993;34(14):2975–80.
[7] Barham PJ, Hill MJ, Goldbeck-Wood G, van Ruiten J. Polymer 1993;34(14):2981–8.
[8] Hill MJ, Barham PJ. Polymer 1994;35(9):1802–8.
[9] Alamo RG, Londono JD, Mandelkern L, Stehling FC, Wignall GD. Macromolecules 1994;24:411–7.
[10] Alamo RG, Graessley WW, Krishnamoorti R, Lohse DJ, Londono JD, Mandelkern L, Stehling FC, Wignall GD. Macromolecules 1997;30:561–6.
[11] Agamalian M, Alamo RG, Kim MH, Londono JD, Mandelkern L, Wignall GD. Macromolecules 1999;32:3093–6.
[12] Morgan RL, Hill MJ, Barham PJ. Polymer 1999;40:337–48.
[13] Schweizer KS, David EF, Singh C, Curro JG, Rajasekaran JJ. Macromolecules 1995;28:1528–40.
[14] Schweizer KS, Singh C. Macromolecules 1995;28:2063–80.
[15] Rajasekaran JJ, Curro JG, Honeycutt JD. Macromolecules 1995;28:6843–53.
[16] Choi P, Blom H, Kavassalis TA, Rudin A. Macromolecules 1995;28:8247–50.
[17] Maranas JK, Mondello M, Grest GS, Kumar SK, Debenedetti PG, Graessley WW. Macromolecules 1998;31:6991–7.
[18] Maranas JK, Kumar SK, Debenedetti PG, Graessley WW, Mondello M, Grest GS. Macromolecules 1998;31:6998–7002.
[19] Paul DR, Newman S. In: Paul DR, Newman S, editors. Polymer Blends, New York: Academic Press, 1979.
[20] Schweizer KS, Curro JG. In: Prigogine I, Rice SA, editors. Advances in chemical physics, XCVIII. New York: Wiley, 1997. p. 65–7.
[21] Colbourn EA. In: Colbourn EA, editor. Computer simulation of polymers, London: Longman, 1994.
[22] Theodorou D, Suter U. Macromolecules 1985;18:1467–78.
[23] Rudin A, Chee KK, Shaw JH. J Polym Sci: Part C 1970;30:415–27.
[24] Flory PJ. Statistical mechanics of chain molecules. New York: Oxford University Press, 1988 chap. 3.
[25] Allen MP, Tildesley DJ. Computer simulation of liquids. Oxford: Oxford University Press, 1987.
[26] Mayo SL, Olafson BD, Goddard III WA. J Phys Chem 1990;94:8897–909.
[27] Choi P, Kavassalis TA, Rudin A. J Colloid Interf Sci 1992;150:386–93.
[28] Kavassalis TA, Choi P, Rudin A. Molecular Simulation 1993;11(2-4):229–41.
[29] Choi P, Kavassalis TA, Rudin AI. EC Research 1994;33:3154–9.
[30] Choi P. PhD thesis, University of Waterloo, 1995.
[31] Han SJ, Lohse DJ, Condo PD, Sperling LH. J Polymer Sci: Part B 1999;37:2835–44.
[32] Mondello M, Grest GS. J Chem Phys 1995;103(16):7156–65.
[33] Sun H, Rigby D. Spectrochimica Acta: Part A 1997;53:1301–23.
[34] Sun H. J Phys Chem B 1998;102:7338–64.
[35] Nosé S. J Chem Phys 1984;81:511–9.
[36] Kavassalis TA, Choi P, Rudin A. In: Gubbins KE, Quirke N, editors. Methods, examples and prospects, Molecular simulation and industrial applications, Amsterdam: Gordon and Breach, 1996. p. 315–29.
[37] Graessley WW, Krishnamoorti R, Balsara NP, Fetters LJ, Lohse DJ, Schulz D, Sissano J. Macromolecules 1994:2574–9 (see also p. 3073–81, 3896–901).
[38] Graessley WW, Krishnamoorti R, Reichart GC, Balsara NP, Fetters LJ, Lohse DJ. Macromolecules 1995;28:1260–70.
[39] Krishnamoorti R, Graessley WW, Fetters LJ, Garner RJ, Lohse DJ. Macromolecules 1995;28:1252–9.
[40] Taylor JR. An introduction to error analysis, The study of uncertainties in physical measurements. Mill Valley: University Science Book, 1982 (chap. 3).